The Validation of a Compression Testing Method for Cancellous Human Jawbone by High-resolution Finite Element Modeling

Nele Stoppie, DDS[1]/Tim Van Cleynenbreugel, M Sc Eng, PhD[2]/Martine Wevers, M Sc Eng, PhD[3]/
Jos Vander Sloten, M Sc Eng, PhD[4]/Ignace Naert, DDS, PhD[5]

Purpose: *The aim of this study was to determine a reliable compression testing method for cancellous jawbone specimens and to validate it by high-resolution finite element (FE) modeling based on micro-computerized tomography (μCT) images of the specimens.* ***Materials and Methods:*** *Three series of human femoral bone samples were tested to establish a compression protocol for human jawbone cores. A μCT scan of each bone sample was obtained. A simple destructive compression test was performed on the first series of 12 femoral bone samples (13 mm height and 6.1 mm diameter). The 5 femoral bone samples of the second series (13 mm height and 6.1 mm diameter) were constrained using end caps and subjected to 10 to 15 conditioning cycles before the destructive test from which the Young's modulus (E_{meas}) was determined. The third series of 5 smaller femoral samples (8 mm height and 5.5 mm diameter) and the series of 5 jaw bone samples (8 mm height and 5.7 mm diameter) underwent the same testing protocol. FE models were created based on the μCT images, and the simulated E-modulus (E_{calc}) was calculated.* ***Results:*** *The intraclass correlation between E_{meas} and E_{calc} corresponded to 0.74 for the first series of femoral bone samples, 0.96 for the second series, and 0.51 for the third series. For the jawbone samples, the intraclass correlation coefficient equaled 0.88.* ***Conclusion:*** *Reliable results for compression testing of cancellous jawbone can be obtained with cylindric specimens with a diameter of 5.7 mm, a length:diameter ratio 1.4, and flat top and bottom surfaces. The recommended compression method is constrained compression with 10 to 15 conditioning cycles, followed by a destructive test.* INT J ORAL MAXILLOFAC IMPLANTS 2007;22:436–445

Key words: *cancellous bone, compression, finite element modeling, jaws, micro-computerized tomography*

Finite element (FE) models are commonly used in implant dentistry to predict the effect of implant geometry, prosthesis design, and type of loading on the stress and strain distribution in the peri-implant region. These models require the input of elastic moduli of cancellous and cortical jawbone; this information is generally obtained by compression testing. Cancellous bone is a difficult material to test mechanically. However, jawbone is not a homogeneous tissue. There can be enormous variation in strength within an anatomic site. Second, cancellous bone is anisotropic; great differences in stiffness may exist in different directions within the same anatomic location. Furthermore, cancellous bone is viscoelastic, ie, the stress developed within bone is dependent on the rate at which the bone is strained. With increasing strain rates, the bone appears stiffer and stronger.[1] These properties make it difficult to test cancellous bone in a reliable way. This may be one reason for the small number of articles published on the mechanical testing of cancellous jawbone specimens.[2,3] Keaveny et al[4] performed a theoretical analysis of the effect of bone specimen geometry on Young's modulus underestimation. The conclusion was that more accurate

[1]Assistant Professor, Department of Prosthetic Dentistry/BIOMAT Research Group, School of Dentistry, Oral Pathology and Maxillofacial Surgery, Katholieke Universiteit Leuven, Belgium.
[2]Research Fellow, Division of Biomechanics and Engineering Design, Department of Mechanical Engineering, Katholieke Universiteit Leuven, Belgium.
[3]Full Professor, Department of Metallurgy and Materials Engineering, Katholieke Universiteit Leuven, Belgium.
[4]Full Professor and Chairman, Division of Biomechanics and Engineering Design, Department of Mechanical Engineering, Katholieke Universiteit Leuven, Belgium.
[5]Full Professor and Chairman, Department of Prosthetic Dentistry/BIOMAT Research Group, School of Dentistry, Oral Pathology and Maxillofacial Surgery, Katholieke Universiteit Leuven, Belgium.

Correspondence to: Dr Ignace Naert, Department of Prosthetic Dentistry/BIOMAT Research Group, Kapucijnenvoer 33, 3000 Leuven, Belgium. Fax: +0032 16 33 23 09. E-mail: ignace.naert@med.kuleuven.be.

predictions of modulus and strength can be obtained using cylindric bone specimens with a 2:1 length:diameter ratio. A cylindric specimen 5 mm in diameter and 10 mm in length was recommended for compression testing of human cancellous bone.[5] In the human maxilla and mandible, these dimensions cannot be attained because of the small amount of cancellous bone present. A length:diameter ratio of 1 is generally used. O'Mahony et al[3] were the first to report elastic moduli for the cancellous bone from the edentulous mandible in 3 orthogonal directions and to relate these values to apparent density and volume fraction. Small cubes with a length:diameter ratio of 1 were tested. It appeared difficult to obtain good samples because of the weakness of the cancellous jawbone after removal of the cortex. Detailed data on the elastic properties of cancellous bone from the dentate mandible and from the dentate or edentulous maxilla are still lacking. Before new mechanical tests can be performed to define these values, it is necessary to investigate the method of compression testing for jawbone specimens with their specific dimensions.

The aim of this study was to find a reliable compression testing method for the evaluation of cancellous jawbone specimens and to validate this compression technique by means of FE modeling based on micro-computerized tomography (μCT) images. For this purpose, different methods of compression testing were first tried on femoral bone samples of different dimensions and were validated afterward by FE modeling. Next, jawbone samples underwent the chosen testing protocol and analysis.

MATERIALS AND METHODS

Cancellous Bone Samples

Three series of human femoral bone were tested to define the final compression protocol of the series of human jawbone cores.

Human Femoral Bone. Cancellous bone cores were obtained from a fresh frozen human femur (age and gender unknown). With an Exakt band saw (Exakt-Trenn-schleifsystem-Makro; Exakt Apparatebau, Norderstedt, Germany) slices either 8 or 13 mm thick were cut from the femoral head. Care was taken to ensure that top and bottom surfaces of the slices were parallel. Using a trephine bur (Biomet 3i, Palm Beach Gardens, FL) with an inner diameter of 6 mm, the samples were drilled from the slices. The samples were frozen and stored in a freezer at –20°C. A total of 17 specimens 6.1 mm in diameter and 13 mm high and 5 specimens of 5.5 mm in diameter and 8 mm high were prepared.

Human Jawbone. Twenty-four bone samples were obtained from 8 embalmed jaws (5 maxillae and 3 mandibles) within the framework of a larger study.[6] The details of the jawbone sample preparation are described in this previous study. Surgical drill guides based on stereolithographic models of the jaws were made for trephination of the bone samples at the preselected sites (Materialise, Haasrode, Belgium). The bone samples were retrieved with a trephine bur (6 mm inner diameter) under perfuse cooling for the full height of the jaw, perpendicular to the occlusal plane. To remove the upper and lower cortices, the samples were frozen with liquid nitrogen into a holder 8 mm in height. A Stäubli robot (Stäubli RX 130, 6 degrees of freedom; Stäubli Unimation, Faverges, France) was used to mill the ends of the bone samples to obtain an exact height of 8 mm. The cylindric bone samples were stored in saline solution in a freezer at –20°C. A total of 24 specimens 5.7 mm in diameter and 8 mm high were prepared.

μCT Scanning

Each sample was scanned in the Skyscan 1072 μCT system (Skyscan, Aartselaar, Belgium). The settings of the x-ray source were a voltage of 50 kV and a current of 300 μA. The resulting cross-sectional images were 8-bit grayscale bitmaps of 1024 × 1024 pixels with a pixel size and interslice distance of 13.67 μm. The μCT images showed that all the femoral bone samples were composed solely of cancellous bone. In contrast, of the 24 jawbone specimens, 13 specimens were a mix of cancellous and cortical bone. Eleven jawbone specimens were composed of cancellous bone only.

Mechanical Testing

Six hours prior to testing, the samples were removed from the freezer and allowed to thaw at room temperature. The compression test was performed on an Instron 4467 mechanical testing machine (Instron, High Wycombe, England). A load cell with a range of up to 1 kN was used. The specimens were placed on a spherical-seated bearing block resting on the lower compression plate of the testing machine, in correspondence with the standard test method for compression testing of materials (ASTM E9-89a). Three series of femoral bone samples were tested before testing of the jawbone specimens commenced.

First Series of Femoral Bone. Twelve femoral bone samples (diameter, 6.1 mm; height, 13 mm) were removed from a container of physiologic fluid just before testing, and excessive fluid was removed. A simple destructive compression at a constant displacement rate (5 mm/min) was performed. The displacement of the crosshead of the compression machine was measured.

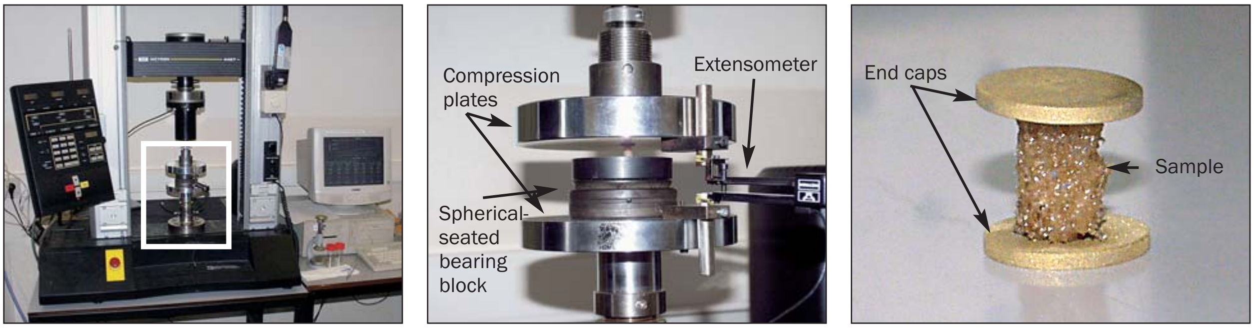

Fig 1 The setup of compression testing for series 2 and 3 of the femoral bone and jawbone specimens.

Second Series of Femoral Bone. In the second series, 5 cancellous femoral bone samples (diameter, 6.1 mm; height, 13 mm) were tested, but precautions were taken to increase the accuracy of the testing.[7] Instead of using the crosshead displacement of the machine, an external extensometer was mounted between the endplates of the machine close to the test specimen. After the samples were removed from the container, brass cylindric disks (end caps) 10 mm in diameter and 1 mm thick were luted to the tops and bottoms of the samples using cyanoacrylate glue (Fig 1). A manual compression device with perfectly parallel plates ensured parallelism of the end caps. Before mechanical testing, a small preload of 3 N was applied to ensure contact between the endplates and the specimen. A lower compression speed (0.2 mm/min) than in the first series was chosen to further eliminate the influence of the viscoelastic behavior of the bone samples. Then the bone specimens were subjected to 10 to 15 conditioning cycles until the structure reached a steady state. This was verified by the inspection of consecutive force-displacement curves. Before each cycle, the strain was set to zero, and the downward movement of the conditioning cycles was controlled until a maximum strain of 0.6% was reached. The upward movement was controlled until a contact force of 3 N was reached. At the steady state, a destructive compression was performed with the same compression speed. The highest slope of the polynomial fitted to the stress-strain curves was considered the Young's modulus (E_{meas}).[7]

Third Series of Femoral Bone. A third series of 5 smaller femoral cancellous bone samples were tested. The samples had a diameter of 5.5 mm and a height of 8 mm, similar to the jawbone specimens. The same testing protocol described for the second series was used for these 5 femoral samples.

Jawbone Series. Only 11 of the 24 jawbone samples were composed of cancellous bone alone. By combining the results from the FE analyses with those of the compression test, it was possible to estimate the bulk E-modulus (the elastic modulus determined by the material) of the trabecular bone tissue. However, a sufficient number of bone specimens is needed from the same jaw in order to estimate the bulk E-modulus of this jaw more accurately. Therefore, 5 jawbone specimens harvested from the same edentulous maxilla were selected. The same testing protocol described for the second series of femoral bone was used for these 5 jawbone samples.

Image Processing and FE Modeling

The image datasets were converted to hexahedron FE meshes. In order to limit the computational requirements, the image datasets were interpolated with a higher voxel size than the original pixel size of the µCT images (13.67 µm). For the cancellous bone samples analyzed (8 to 13 mm in height and 5.3 to 6.2 mm in diameter, with volume fractions [bone volume over total volume, or BV/TV] of 10% to 40%), voxel sizes of 35 to 50 µm were chosen, which was sufficiently small to ensure accurate results. After interpolation, a fixed threshold was visually selected for separation of the bone from the void. Based on the binary datasets, 2 structural parameters were calculated for every bone sample: the average diameter of the sample and the volume fraction.

An axial compression that caused an apparent vertical strain of –1,000 µstrain was applied to the FE models. This was achieved by imposing a vertical displacement on the top nodes of the model and fixing the vertical displacement of the bottom nodes. In the first test series, no end caps were used, and frictionless contact between the sample surfaces and the compression plates was simulated (frictionless compression). In the second and third series, end caps were glued to the top and bottom surfaces of the samples before compression. This corresponded to embedded boundary conditions (constrained compression).

The trabecular bone was modeled as a homogeneous, isotropic material. Initially, a trabecular bulk E-modulus of 1 GPa and a Poisson's ratio of 0.3 were assigned to the bone elements in the FE model. The E-modulus of a bone specimen is determined by the bone from which the sample has been harvested (the bulk E-modulus) and the 3-dimensional architecture of the specimen. After calculation of the E-modulus for a bulk E-modulus of 1 GPa (E_{calc}^{1GPa}), the comparison with the measured E-modulus (E_{meas}) allowed for every bone sample the calculation of the "real" bulk E-modulus (E_{bulk}), which formed a perfect match between the measurement and the simulation for that bone sample ($E_{bulk} = E_{meas} / E_{calc}^{1GPa}$). This was possible because a linear FE analysis was used.

Comparison of Measured and Calculated E-moduli

For each series of bone specimens, the average bulk E-modulus (E_{bulk}^{av}) for all samples in the series was calculated. Since all samples in each series came from the same location in the same bone, it is safe to assume that the bulk E-modulus of the trabecular bone tissue was constant over all samples. Using this E_{bulk}^{av} for all samples in the series, their simulated E-modulus (E_{calc}) was calculated as

$$E_{calc} = \frac{E_{calc}^{1GPa}}{1GPa} \cdot E_{bulk}^{av}$$

Statistical Analysis

To approximate agreement between the 2 methods, E_{meas} and E_{calc} were plotted together with the identity line. If the 2 methods (compression testing and FE modeling) were 100% in agreement, then all points would lie on the identity line.

To assess graphically the agreement between the measured stiffness (E_{meas}) and calculated stiffness (E_{calc}), Bland-Altman plots were calculated. These graphs showed the differences between E_{meas} and E_{calc} plotted against their average. The intraclass correlation (ICC) between E_{meas} and E_{calc} and the corresponding 95% confidence intervals (CIs) were calculated for each series of bone specimens in SAS 8.2 using the MIXED procedure. The ICC assessed the reliability of the methods by comparing the variability of the different methods on the same subject to the total variation. ICC was examined to determine whether measurement of stiffness by compression (E_{meas}) could be replaced by stiffness calculated by FE modeling (E_{calc}). Finally the power correlation between the volume fraction (BV/TV), E_{calc} and E_{meas} was determined. The level of significance was set at .05 for all statistical tests.

RESULTS

Figure 2 demonstrates the scatterplots of E_{meas} and E_{calc} together with the identity line. Figure 3 shows the Bland-Altman plots for the 4 series of bone specimens. These plots demonstrate that there was reasonable agreement between the 2 methods. Table 1 shows the ICC between E_{meas} and E_{calc} for each series of bone specimens with their 95% CIs.

First Series of Femoral Bone

Table 2 summarizes the calculated diameter and volume fraction of the 12 cancellous bone samples in the first test series. An E_{bulk}^{av} of 2,813 MPa was found. Figures 4a and 4b show E_{meas} and E_{calc} versus the volume fraction. For both graphs, the power regression was calculated. For E_{meas} versus BV/TV (Fig 4a), a power of 1.18 was found, with an R^2 of 0.77. For E_{calc} versus BV/TV (Fig 4b), a power of 1.87 was obtained with an R^2 of 0.97.

Second Series of Femoral Bone

Table 3 summarizes the calculated diameter and volume fraction (BV/TV) of the 5 cancellous femoral bone samples in the second test series. The range of volume fractions for the samples in the second series was very narrow; volume fractions between 16.5% and 19% were measured. The narrowness of this range would have caused the correlation between volume fraction and measured or calculated stiffness to be very poor. For this reason, these correlations were not calculated. E_{bulk}^{av} was 5,900 MPa.

Third Series of Femoral Bone

Table 4 summarizes the calculated diameter and volume fraction of the 5 cancellous bone samples in the third series. Due to the small range of volume fractions (10.5% to 16.4%), the correlations between the volume fraction and measured or calculated stiffness were not calculated. E_{bulk}^{av} was 3,366 MPa.

Jawbone Series

Table 5 summarizes the calculated diameter and volume fraction (BV/TV) of the 5 cancellous jaw bone samples. Figures 5a and 5b, respectively, show E_{meas} and E_{calc} versus the volume fraction (BV/TV). For both, the power regression was calculated. For E_{meas} (Fig 5a), a power of 1.97 was found, with an R^2 of 0.94. For E_{calc} (Fig 5b), a power of 1.84 was obtained, with an R^2 of 0.82. E_{bulk}^{av} was 3,520 MPa.

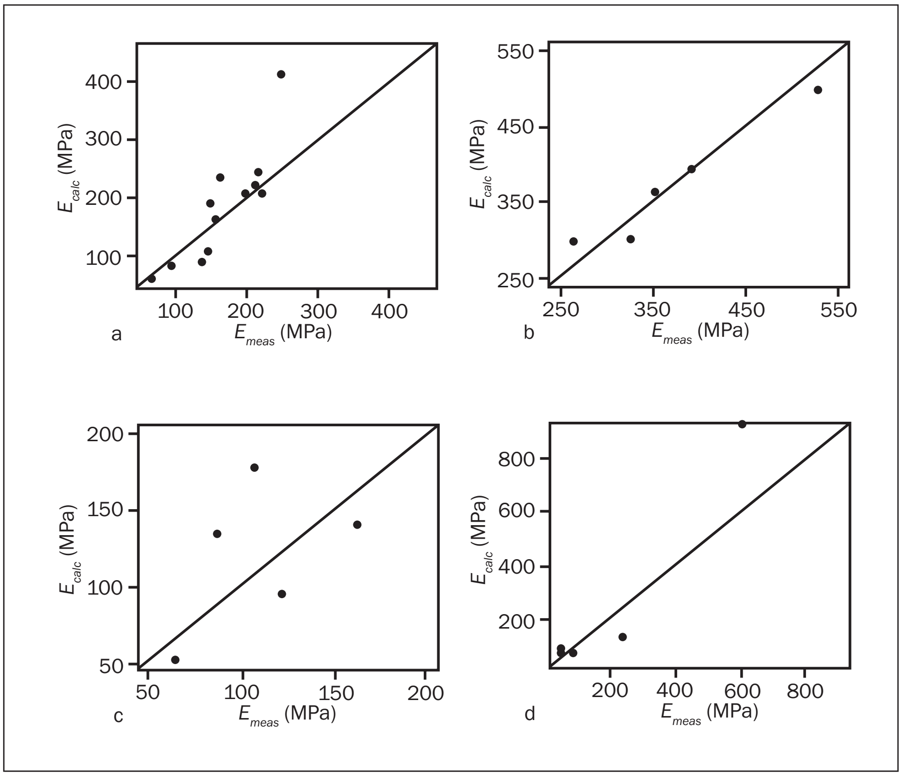

Fig 2 The scatter plots of E_{meas} and E_{calc} together with the identity line for *(a)* the first series of femoral bone, *(b)* the second series of femoral bone, *(c)* the third series of femoral bone, and *(d)* the jawbone series.

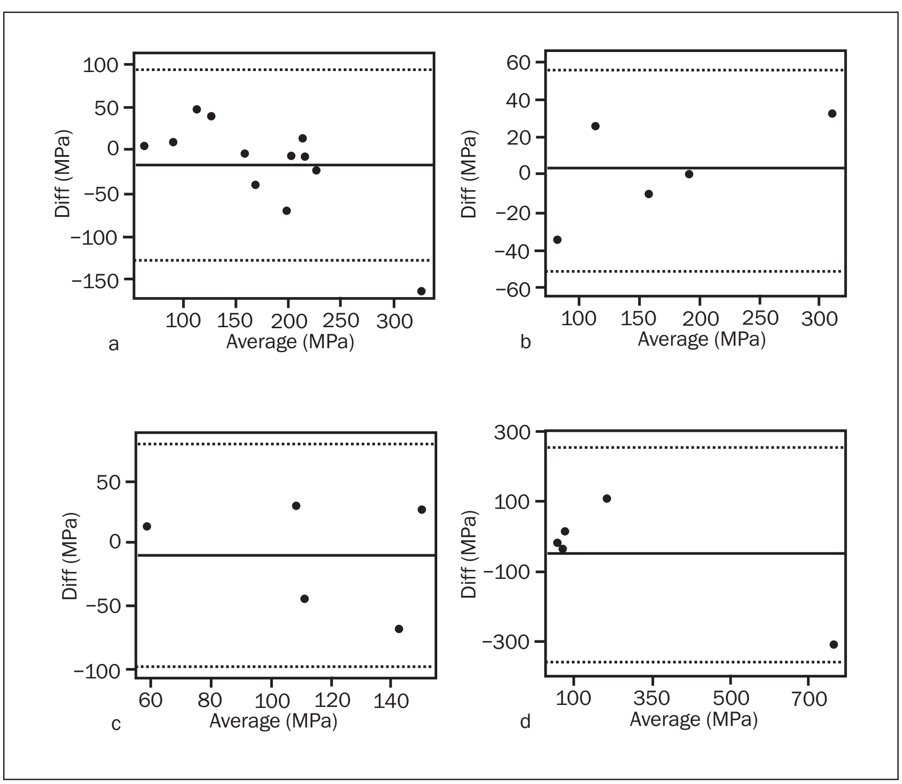

Fig 3 The Bland-Altman plots showing the differences between E_{meas} and E_{calc} plotted against their average for *(a)* the first series of femoral bone, *(b)* the second series of femoral bone, *(c)* the third series of femoral bone, and *(d)* the jawbone series.

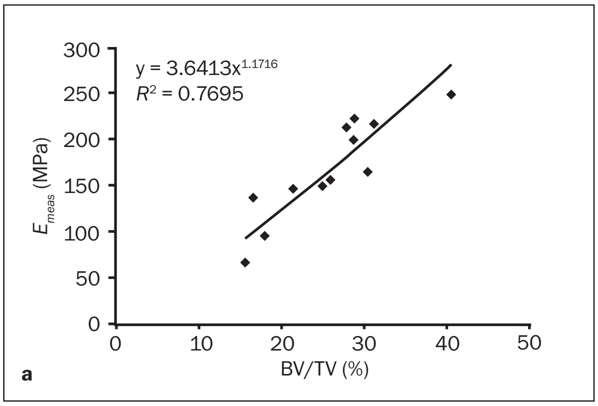

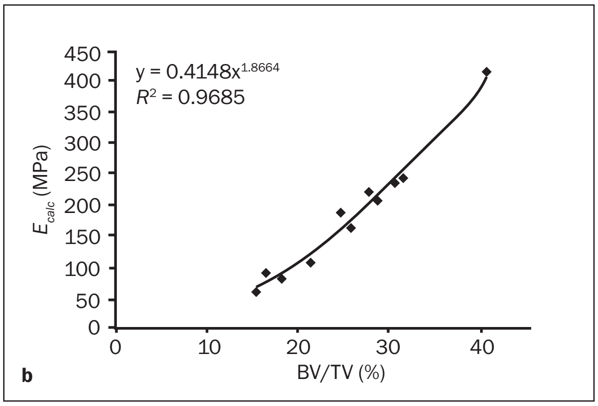

Fig 4 *(a)* The measured stiffness E_{meas} and *(b)* the calculated stiffness (E_{calc}) versus volume fraction (BV/TV) of the femoral bone samples in the first series. Power regression and corresponding R^2 are shown.

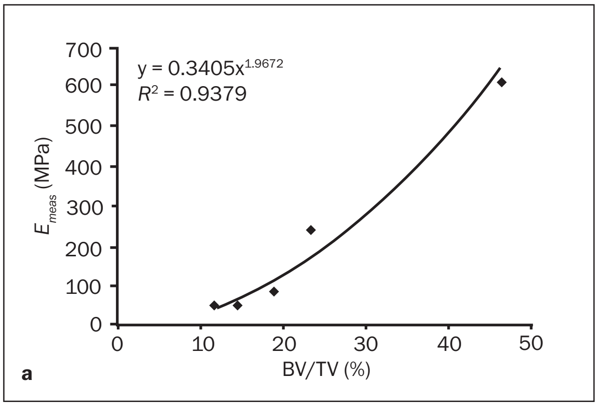

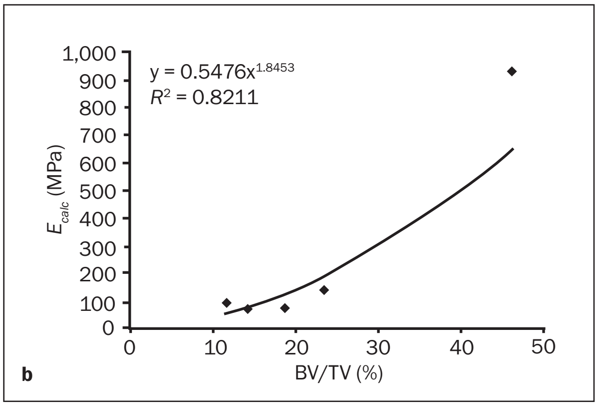

Fig 5 *(a)* The measured stiffness (E_{meas}) and *(b)* the calculated stiffness (E_{calc}) versus volume fraction (BV/TV) of the jawbone samples. Power regression and corresponding R^2 are shown.

Table 1 ICC Between E_{meas} and E_{calc} for Each Series of Bone Specimens with 95% CIs

				95% CI	
Bone	**Series**	**ICC**	**SE**	**Lower**	**Upper**
Femoral	1	0.738	0.135	0.474	1
Femoral	2	0.964	0.034	0.898	1
Femoral	3	0.513	0.349	0	1
Jaw		0.882	0.105	0.676	1

SE = standard error.

Table 2 Diameter and Volume Fraction (BV/TV) of the Femoral Bone Samples

Sample	Diameter (mm)	BV/TV (%)
1-1	6.12	27.94
1-2	6.09	25.83
1-3	6.04	18.19
1-4	6.08	15.54
1-5	6.10	30.61
1-6	6.07	24.89
1-7	6.04	16.52
1-8	6.18	31.44
1-9	6.04	21.46
1-10	6.08	28.78
1-11	6.18	28.73
1-12	6.16	40.67

Table 3 Diameter and Volume Fraction (BV/TV) of the Femoral Bone Samples in the Second Series

Sample	Diameter (mm)	BV/TV (%)
2-1	6.06	18.29
2-2	6.09	16.97
2-3	6.05	16.56
2-4	6.04	18.46
2-5	6.11	18.95

Table 4 Diameter and Volume Fraction (BV/TV) of the Femoral Bone Samples in the Third Series

Sample	Diameter (mm)	BV/TV (%)
3-1	5.54	13.16
3-2	5.35	15.33
3-3	5.69	16.36
3-4	5.91	10.58
3-5	5.24	11.57

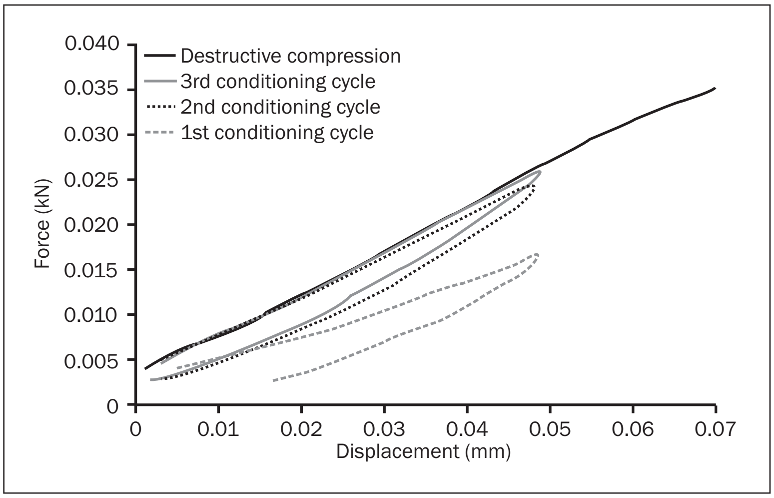

Fig 6 Force-displacement curves measured during the conditioning cycles and consecutive destructive compression of a cancellous bone sample. The stiffening during the conditioning cycles is clearly visible.

Table 5 Diameter and Volume Fraction (BV/TV) of the Jawbone Samples

Sample	Diameter (mm)	BV/TV (%)
1	5.47	11.76
2	5.49	18.95
3	6.06	46.25
4	5.94	23.40
5	5.51	14.40

DISCUSSION

First Series of Femoral Bone

In the mechanical testing of the first series, no end caps were used. This corresponded to frictionless boundary conditions in the FE analyses. However, in reality it is very hard to achieve perfect frictionless contact between the bone surface and the compression plates. Other sources of inaccuracies during the mechanical testing of cancellous bone samples were the viscoelastic behavior of bone tissue and small surface irregularities of the specimen surfaces. These caused the measured stiffness of the bone sample to be an underestimation. Linde and Hvid[7] reported the net result of systematic errors to be an underestimation of the stiffness of 20% to 40%. This explained why an E_{bulk}^{av} of 2,813 MPa was found, which is a low value for the stiffness of trabecular bone tissue. Zysset et al[8] found elastic moduli of 6.9 ± 4.3 GPa in trabecular bone tissue from the femoral neck using nanoindentation.

However, despite these sources of inaccuracy relatively good results were obtained when comparing the measured and calculated stiffness of the cancellous bone samples (Fig 2). An ICC of 0.74 was calculated (Table 1). This relatively high value can be explained by the fact that the underestimation of the stiffness affected all samples of the first series in a systematic way.

The correlation between the calculated stiffness and the volume fraction was better (R^2 = 0.97) than that between the measured stiffness and the volume fraction (R^2 = 0.77). According to Rice et al,[9] the apparent E-modulus of cancellous bone is proportional to the square of the volume fraction. For the calculated stiffness, a power of 1.87 was found. This is much closer to 2 than the power found for the measured stiffness, which was 1.17. The results suggested that the stiffness calculation using high-resolution FE models of cancellous bone was more accurate than the stiffness measurements using a mechanical compression test.

Second Series of Femoral Bone

For the samples in the second series, precautions were taken to minimize inaccuracy during compression testing. The use of an extensometer ensured that deformation was measured more accurately. Testing machines driven by 2 screws moving the crosshead up and down often produce an extra loop due to a small tilting of the crosshead when the machine turns from loading to unloading. This is especially important when using small displacements, for example, during the conditioning cycles. The luting of end caps eliminated irregularities at the cut bone surfaces. Also the influence of the structural end phenomena caused by the cutting of trabeculae was minimized. Another advantage was that the testing conditions corresponded better with FE boundary conditions.[10] The use of brass disks decreased the friction between the steel machine compression plates and the end caps. The conditioning cycles minimized the viscoelastic influence on the stiffness and smoothed out small surface irregularities. Figure 6 shows the force-displacement curves during the conditioning cycles and the consecutive destructive compression of a cancellous bone sample. A stiffening of the structure during the conditioning cycles can be observed. All these precautions caused the results of the second series to be better than the first series. Table 1 showed that excellent agreement existed between the measured and calculated stiffness for this series; an ICC of 0.96 was found. E_{bulk}^{av} was 5,900 MPa. This value is well within the range reported by Zysset et al.[8] These results proved that the described method of compression testing was reliable since FE modeling based on µCT images could accurately simulate it.

Third Series of Femoral Bone

The most popular specimen geometries for compression testing are cubes and cylinders. Keaveny et al[4] argued against the use of a cubic specimen geometry as a standard in biomechanical testing, because cylinders can be made more easily and accurately than cubes. The surface-to-volume ratio is lower for cylinders than for cubes of the same aspect ratio, which permits more accurate density measurement. More accurate predictions of the Young's modulus were found with cylinders with a 2:1 aspect ratio than with cubes of the same width.[4] For these reasons, the cylinder was chosen instead of the cube as specimen geometry in this study.

The specimen diameter should be large enough to satisfy continuum scale assumptions but at the same time small enough to ensure specimen homogeneity. Keller and Liebschner[5] recommended a 5-mm-diameter cylindric specimen with an aspect ratio of 2:1 for optimal compression testing of cancellous bone. In this study, a hollow cylindric drill was used. The same drill was used for series 1 and 2 of the femoral bone. The drill was then changed for series 3 of the femoral bone and the jawbone specimens because of decreased sharpness. For series 1 and 2, the average diameter of the samples was 6.1 mm (Tables 2 and 3). For series 3 and the jawbone series, the samples had average diameters of 5.55 mm (Table 4) and 5.69 mm (Table 5), respectively. Differences in the bone quality can explain this difference in mean diameter. In the jaw it was difficult to obtain cancellous bone specimens with a height of 10 mm; a maximum of 8 mm was achievable. Thus, in the third series of femoral bone samples, the length:diameter ratio was 1.4 (8 mm length and 5.5 mm diameter).

Exactly the same mechanical testing protocol was used for series 2 and 3. One would therefore expect the similarly accurate results for the 2 series, as the only difference was the smaller height:diameter ratio. The samples in the first and second series had a length:diameter ratio of 2.2 (13 mm length and 6 mm diameter). However, in contrast to the results of series 2, a lack of agreement existed between the measured and calculated stiffness; an ICC of 0.51 was calculated (Table 1). Also the E_{bulk}^{av} calculated from all 5 femoral bone samples was 3,366 MPa, which is low for trabecular bone tissue. The standard deviation of 1,146 MPa indicated a very wide spread of the individual E_{bulk}.

In order to find the cause of these anomalous results, the µCT images of the samples were studied more closely. This revealed that samples 3-2 and 3-3 demonstrated structural imperfections in their top surfaces (Fig 7). The top surface of sample 2 was very uneven; one half of the surface was higher than the other. In the top part of sample 3, a large part was missing. During the FE modeling, surface irregularities at the top and bottom were virtually "cut" from the model by using only those images from the image data set that contained the complete cross section. This caused the FE model to have a flat top and bottom surface, which facilitated the implementation of boundary conditions corresponding to axial compression. In reality, the top parts of the specimens were less stiff during compression, but this was not modeled. As a consequence, the FE simulation overestimated the apparent stiffness. The E_{bulk} of both samples was therefore largely underestimated, which explains the low E_{bulk}^{av} and large standard deviation.

Jawbone Series

Of the 11 jawbone samples that consisted of purely cancellous bone, a need for parallelism and the condition of equal origin resulted in the selection of 5 jawbone samples with flat surfaces from the same edentulous maxilla.

The jawbone specimens in this study were embalmed, which increased collagen cross-linking and therefore altered the properties of the bone tissue. Evans[11] reported that embalming caused a 68% increase in Young's modulus and ultimate tensile strength. McElhaney et al[12] found a 6% decrease of the compressive modulus with embalming. Although the results of these 2 studies were equivocal, they both indicated that embalming dramatically alters the mechanical behavior of bone. However, the focus of this study was not to obtain values of stiffness of cancellous bone in the jaw but to establish a reliable method of compression testing to determine these values in the near future. Therefore, the use of embalmed specimens was justified, since a fixed decrease or increase of Young's modulus would not alter the correlation with other parameters. For the jawbone specimens, good agreement was found between the measured and calculated stiffness; an ICC of 0.88 was calculated (Table 1).

In this study, the BV/TV for the 5 cancellous maxilla bone samples corresponded with a mean value of 23% (range, 12% to 46%; Table 5). Fanuscu and Chang[13] selected 6 sites in a human cadaveric

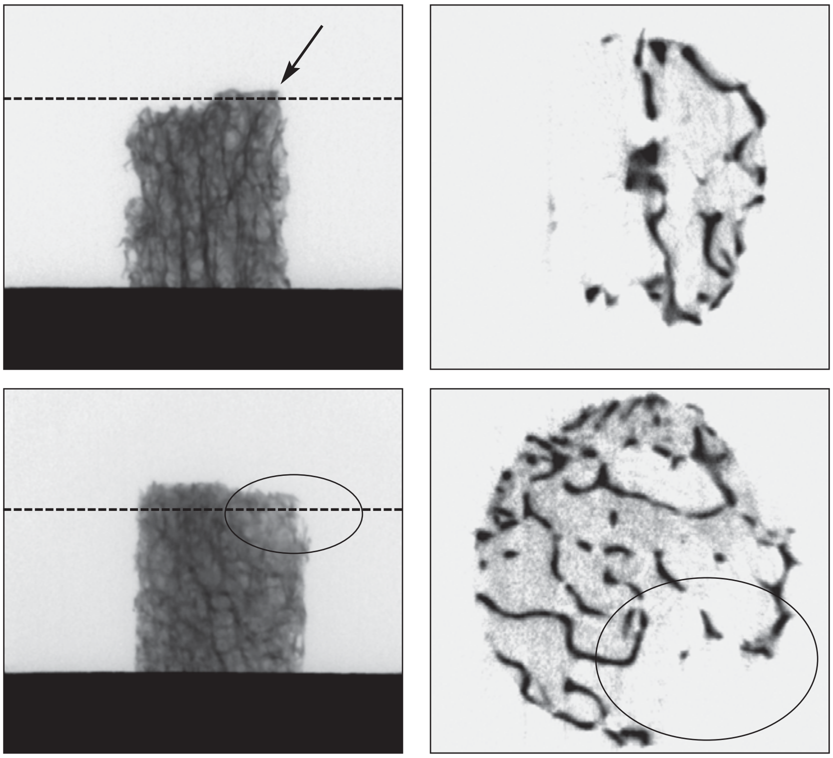

Fig 7 *(Top)* Radiographic image of femoral bone sample 2 from the third series *(left)* and cross section of the top of the sample *(right).* One portion of the upper surface was higher than the rest of the surface *(arrow). (Bottom)* Radiographic image of femoral bone sample 3 from the third series *(left)* and cross section of the top of the sample *(right).* A less dense area is visible *(circle),* indicating a hole in the sample.

mandible and maxilla. BV/TV was determined with µCT scanning, and values of 16% to 29% were found for the 3 maxillary jawbone samples. Nkenke et al[14] found a mean BV/TV of 19.7% (SD 8.8%) for 24 bone samples in the maxilla, based on histomorphometric analysis.

Both for the calculated and measured stiffness (E_{calc} and E_{meas}) the correlation with the volume fraction was calculated using a power model. For the measured stiffness (Fig 5a) and calculated stiffness (Fig 5b), exponents of 1.96 and 1.84 were found, respectively. This was in agreement with the power law of 2 between the E-modulus and the volume fraction, described by Rice et al.[9] These results were in contrast to the power of 1 that O'Mahony et al[3] found between the stiffness and the apparent density of the cancellous bone of the mandible. The main differences between that study[3] and the present study were the specimen geometry and the fact that no end caps were used in the former. O'Mahony et al cut nearly cubic samples of 4.4 × 4.4 × 4.8 mm and used Teflon tape to minimize friction between the sample and the platens. O'Mahony et al,[3] however, agreed that a linear fit between stiffness and apparent density would be unrealistic, since 50% of the variance in their data remained unexplained by a linear fit.

The present study demonstrates that FE models based on µCT images can accurately simulate the described method of constrained compression testing. This validates a new method of obtaining detailed data for the missing elastic properties of cancellous bone from the jaw. A compression test will still be necessary to determine the E_{bulk}^{av} of the jaw, but only a limited number of specimens will have to be used. Once the E_{bulk}^{av} is defined, the stiffness of the bone specimen can be calculated using µCT-based FE modeling.

CONCLUSION

For small samples with a height:diameter ratio of 1.4, surface irregularities can have a significant influence on the results of compression testing. For compression testing of jawbone specimens, this study demonstrated that reliable results can be obtained with cylindric specimens with a length:diameter ratio of 1.4, a diameter of 5.7 mm, and flat, parallel top and bottom surfaces. The recommended compression method is constrained compression with the use of brass end caps, an external extensometer, and 10 to 15 conditioning cycles, followed by a destructive test from which the Young's modulus can be calculated.

ACKNOWLEDGMENTS

This study was supported by the Fund for Scientific Research, Flanders (no. 101/8 and 1.5.118.02, Belgium). Materialise Belgium is acknowledged for providing the planning software and surgical guides.

REFERENCES

1. An YH, Barfield WR, Draughn RA. Basic concepts of mechanical property measurement and bone biomechanics. In: An YH, Draughn RA. Mechanical Testing of Bone and the Bone-Implant Interface. Boca Raton, FL: CRC Press, 2000:23–40.
2. Misch CE, Qu Z, Bidez MW. Mechanical properties of trabecular bone in the human mandible: Implications for dental implant treatment planning and surgical placement. J Oral Maxillofac Surg 1999;57:700–706.
3. O'Mahony AM, Williams JL, Katz JO, Spencer P. Anisotropic elastic properties of cancellous bone from a human edentulous mandible. Clin Oral Implants Res 2000;11:415–421.
4. Keaveny TM, Borchers RE, Gibson LJ, Hayes WC. Theoretical analysis of the experimental artifact in trabecular bone compressive modulus. J Biomech 1993;26:599–607 [erratum 1993;26:1143].
5. Keller TS, Liebschner MAK. Tensile and compression testing of bone. In: An YH, Draughn RA. Mechanical Testing of Bone and the Bone-Implant Interface. Boca Raton, CRC Press, 2000:175–205.
6. Stoppie N, Pattijn V, Van Cleynenbreugel T, Wevers M, Vander Sloten J, Naert I. Structural and radiological parameters for the characterization of jawbone. Clin Oral Implants Res 2006;17:124–133.
7. Linde F, Hvid I. Nondestructive mechanical testing of cancellous bone. In: An YH, Draughn RA. Mechanical testing of bone and the bone-implant interface. Boca Raton, FL: CRC Press, 2000:151–157.
8. Zysset PK, Guo XE, Hoffler CE, Moore KE, Goldstein SA. Elastic modulus and hardness of cortical and trabecular bone lamellae measured by nanoindentation in the human femur. J Biomech 1999;32:1005–1012.
9. Rice JC, Cowin SC, Bowman JA. On the dependence of the elasticity and strength of cancellous bone on apparent density. J Biomech 1988;21:155–168.
10. Jacobs CR, Davis BR, Rieger CJ, Francis JJ, Saad M, Fyhrie DP. The impact of boundary conditions and mesh size on the accuracy of cancellous bone tissue modulus determination using large-scale finite-element modeling. J Biomech 1999;32:1159–1164.
11. Evans FG. Mechanical properties of bone. Springfield, IL: Charles C. Thomas, 1973:56–60.
12. McElhaney JH, Fogle J, Byars E, Weaver G. Effect of embalming on the mechanical properties of beef bone. J Appl Phys 1964;19:1234–1236.
13. Fanuscu MI, Chang TL. Three-dimensional morphometric analysis of human cadaver bone: Microstructural data from maxilla and mandible. Clin Oral Implants Res 2004;15:213–218.
14. Nkenke E, Hahn M, Weinzierl K, Radespiegel-Tröger M, Neukam FW, Engelke K. Implant stability and histomorphometry: A correlation study in human cadavers using stepped cylinder implants. Clin Oral Implants Res 2003;14:601–609.